

FILE COPY
NO 5

TECHNICAL NOTES

NATIONAL ADVISORY COMMITTEE FOR AERONAUTICS

THE FOLLOWING DOCUMENTS ARE IN THE FILES OF
NATIONAL ADVISORY COMMITTEE FOR AERONAUTICS
LANGLEY MEMORIAL AERONAUTICAL LABORATORY
LANGLEY FIELD, HAMPTON, VIRGINIA

RETURN TO THE ABOVE ADDRESS.

No. 825

REQUESTS FOR PUBLICATIONS SHOULD BE ADDRESSED
AS FOLLOWS:

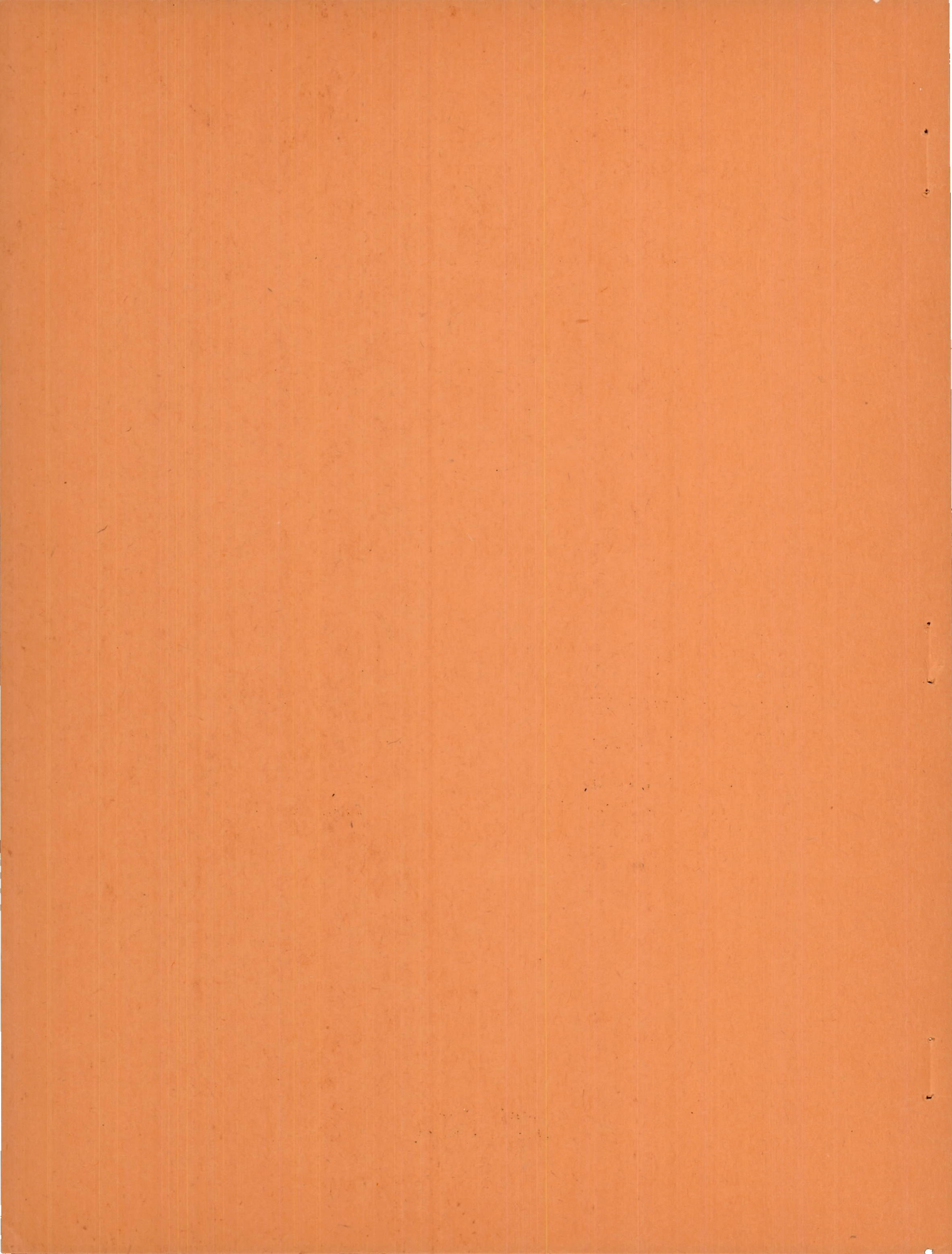
NATIONAL ADVISORY COMMITTEE FOR AERONAUTICS
STREET, N.W.,
WASHINGTON 25, D.C.

WIND-TUNNEL INVESTIGATION OF EFFECT OF YAW ON
LATERAL-STABILITY CHARACTERISTICS

III - SYMMETRICALLY TAPERED WING AT VARIOUS POSITIONS ON
CIRCULAR FUSELAGE WITH AND WITHOUT A VERTICAL TAIL

By Isidore G. Recant and Arthur R. Wallace
Langley Memorial Aeronautical Laboratory

Washington
September 1941



NATIONAL ADVISORY COMMITTEE FOR AERONAUTICS

TECHNICAL NOTE NO. 825

WIND-TUNNEL INVESTIGATION OF EFFECT OF YAW ON
LATERAL-STABILITY CHARACTERISTICS

III - SYMMETRICALLY TAPERED WING AT VARIOUS POSITIONS ON
CIRCULAR FUSELAGE WITH AND WITHOUT A VERTICAL TAIL

By Isidore G. Recant and Arthur R. Wallace

SUMMARY

Model combinations of an NACA 23012 tapered wing and a circular fuselage were tested in the NACA 7- by 10-foot wind tunnel to determine the effect of longitudinal wing position on the change in lateral stability due to interference. The aerodynamic center of the wing was located at approximately 80, 130, and 180 percent of the mean chord from the nose of the fuselage. At each of these locations, the model was tested as a high-wing, a midwing, and a low-wing monoplane. For each combination, tests were made with a partial-span split flap neutral and deflected 60° and with and without a vertical tail. The rearmost low-wing combination was tested with and without a fillet.

The results are presented in the form of charts showing, for each combination, the increments of the slopes of the curves of the rolling-moment, the yawing-moment, and the lateral-force coefficients against yaw due to wing-fuselage interference. Contours are also given that show the variation at zero angle of attack of these increments with the position of the wing on the fuselage.

The longitudinal position of the wing was found to have very little effect on the wing-fuselage interference as compared with vertical position. The wing-fuselage interference tended in most cases to decrease the effective dihedral as the wing position was changed longitudinally; of the three longitudinal locations tested, the maximum effective dihedral was obtained at the central position. The effect of the wing-fuselage interference on directional stability increased favorably when the

wing location was moved forward. The influence of wing-fuselage interference on the directional stability contributed by the vertical tail was beneficial for the low-wing combination and detrimental for the high-wing combination and this influence increased as the wing position was moved rearward. The fillet prevented sudden changes in the lateral-stability characteristics of the low-wing model at high angles of attack below the stall by delaying the occurrence of the burble at the wing-fuselage juncture.

INTRODUCTION

The rates of change of rolling-moment, yawing-moment, and lateral-force coefficients with yaw are important factors in the calculation of the lateral stability of an airplane and, consequently, these parameters have been the subject of extensive investigation by the NACA. The effects of such variables as tip shape, dihedral, taper, and sweep are reported in references 1 and 2. A theoretical determination of lateral-stability characteristics of wings as affected by some of these factors is presented in reference 3. The effect of wing-fuselage interference on lateral-stability characteristics has been investigated for wings of various tapers and sweeps in such combinations with circular and elliptical fuselages as to form high-wing, midwing, and low-wing monoplanes. These results are given in references 4 and 5.

The tests reported herein are a continuation of the investigation of wing-fuselage interference and were made with the circular fuselage and symmetrically tapered wing used in the tests described in reference 4. The chief variable was the longitudinal position of the wing on the fuselage. The wing was located one-half of the mean chord length forward and rearward of the position used for the tests of reference 4. At each horizontal location the model was tested as a high-wing, a midwing, and a low-wing monoplane. Data for the central position, taken from reference 4, are included for comparison.

APPARATUS AND MODELS

The tests were made in the NACA 7- by 10-foot wind tunnel with the regular six-component balance. The tunnel and the balance are described in references 6 and 7.

The model (see fig. 1) was the same as the one used for the tests of reference 4, except that the fuselage was recut so that the wing could be mounted about 0.5 of the mean chord forward and about 0.5 of the mean chord rearward of the original position. For the high-wing and the low-wing combinations the outer surface of the wing was made tangent to the surface of the fuselage. In all cases the wing was set at 0° incidence.

The 3:1 symmetrically tapered wing, which is fully described in reference 3, is of NACA 23012 section with the maximum upper surface ordinates in one plane, giving the chord plane a dihedral of 1.45° . The tips are formed of quadrants of approximately similar ellipses. The sweepback of the locus of one-quarter chord points is 4.75° , the area is 4.1 square feet, and the aspect ratio is 6.1.

The fuselage is circular in cross section and was made to the ordinates given in reference 8. The vertical tail is of NACA 0009 section and has an arbitrary area of 53.7 inches, which includes a portion through the fuselage as shown in figure 1. Its aspect ratio, based on this area and the span measured from the center line of the fuselage, is 2.2.

Split flaps of 20-percent chord and 60-percent span were made of 1/16-inch steel. For the high-wing and the midwing combinations, the flaps were cut to allow for the fuselage, and the gaps between the fuselage and the flaps were sealed. The flaps were attached at a 60° setting.

When the wing was in the low rearward position, a fillet was used. The fillet is shown in figures 2(a) and 2(b).

TESTS

The test procedure was similar to that used in previous investigations (references 4 and 5). The wing was tested in the high, the middle, and the low positions at 0.5 of the mean chord both forward and rearward of the longitudinal locations used in reference 4. Tests were made with and without the flaps and with and without the vertical tail for all wing positions.

All combinations were tested at angles of attack

from -10° to 20° with the model yawed -5° , 0° , and 5° . A yaw range of -10° to 15° was investigated at angles of attack 1° and 4° below the angle of attack for maximum lift.

A dynamic pressure of 16.37 pounds per square foot, which corresponds to a velocity of 80 miles per hour under standard conditions, was used in all tests. The Reynolds number based on a mean wing chord of 9.842 inches was about 609,000. Based on a turbulence factor of 1.6, the effective Reynolds number was about 975,000.

RESULTS

The data are given in standard nondimensional coefficient form with respect to the wind axes and the center-of-gravity locations shown in figure 1. The coefficients for the fuselage alone and fuselage plus fin are based on wing dimensions.

- C_L lift coefficient (L/qS)
- C_D drag coefficient (D/qS)
- C_m pitching-moment coefficient ($M/qS\bar{c}$)
- C_Y' lateral-force coefficient (Y'/qS)
- $C_Y' \psi$ slope of curve of lateral-force coefficient against yaw ($\partial C_Y' / \partial \psi'$)
- C_l' rolling-moment coefficient (L'/qSb)
- $C_l' \psi$ slope of curve of rolling-moment coefficient against yaw ($\partial C_l' / \partial \psi'$)
- C_n' yawing-moment coefficient (N'/qSb)
- $C_n' \psi$ slope of curve of yawing-moment coefficient against yaw ($\partial C_n' / \partial \psi'$)
- Δ_1 change in partial derivatives caused by wing-fuselage interference
- Δ_2 change in vertical tail effectiveness caused by wing-fuselage interference

where

L lift
D drag
Y' lateral force
L' rolling moment
M pitching moment
N' yawing moment
q dynamic pressure ($1/2\rho V^2$)
V tunnel air velocity
 ρ air density
S wing area
b wing span
 \bar{c} average wing chord

and

α angle of attack corrected to free stream, degrees
 α' wind-tunnel angle of attack, degrees
 ψ' angle of yaw, degrees
 δ_f angle of flap deflection, degrees

Lift, drag, and pitching-moment coefficients for the various wing-fuselage arrangements are presented in figure 3. The values of α and C_D shown in this figure were corrected to free air, but in all subsequent figures no corrections to α' were made. Plots of rolling-moment, yawing-moment, and lateral-force coefficients for the low-wing combination are given in figures 4 to 6 for yaw tests at 1° and 4° below the angle of attack for maximum lift. The lateral-stability characteristics of component parts of the model appear in figure 7.

The increments of the partial derivatives with respect to ψ' of rolling-moment, yawing-moment, and lateral-force coefficient due to wing-fuselage interference Δ_1 and due to wing-fuselage interference on the vertical tail Δ_2 are shown in figures 8 to 13 and in figures 14 and 15 by contours for $\alpha' = 0^\circ$. The zero value of angle of attack, for which the contours were made, is considered representative because the interference increments do not vary greatly with angle of attack. All data for the central longitudinal wing positions were taken from reference 4. The increment Δ_1 is the difference between the slope for the wing-fuselage combination without the fin and the sum of the slopes for the wing and the fuselage, each tested separately. Thus, Δ_1 is the change in $C_l'\psi$, $C_n'\psi$, and $C_y'\psi$ caused by wing-fuselage interference for the model without the tail. The increment Δ_2 is the difference between the slope produced by the vertical tail with the wing present and the slope produced by the vertical tail with the wing absent. The increment Δ_2 is therefore the change in effectiveness of the vertical tail caused by the addition of the wing to the fuselage. If, for example, the value of $C_n'\psi$ for the complete model is desired, the following equation may be used:

$$C_n'\psi = C_n'\psi (\text{wing}) + C_n'\psi (\text{fuselage and tail}) + \Delta_1 C_n'\psi + \Delta_2 C_n'\psi$$

Values of $C_l'\psi$ and $C_y'\psi$ for the complete model may be obtained in a similar manner.

The values of $C_l'\psi$, $C_n'\psi$, and $C_y'\psi$ used to compute Δ_1 and Δ_2 were obtained from tests at -5° and 5° yaw by assuming a straight-line variation between those points. This assumption has been shown in reference 5 to be valid except at high angles of attack. Tailed points on the curves of figures 8 to 13 were obtained from slopes measured from curves in figures 4 to 6 and others similar to these.

The values of $C_l'\psi$ and $C_n'\psi$ depend on the center-of-gravity location. All data, except as noted, are given about a center-of-gravity location that moved with the wing longitudinally while it remained on the center line of the fuselage. This method is considered to be the most practical because the aerodynamic center of the wing will be in the neighborhood of the center of gravity on airplanes.

It is likely therefore that $\Delta_1 C_n'_{\psi}$, $\Delta_2 C_n'_{\psi}$, $\Delta_1 C_l'_{\psi}$, and $\Delta_2 C_l'_{\psi}$ contain increments due to the movement of the center of gravity with respect to the fuselage. For this reason some of the data were recomputed for a center-of-gravity location fixed at the center position on the fuselage and are presented in figures 9(d), 9(e), 12(d), and 12(e). With the fixed center of gravity, the tail length is the same for all combinations and the effect of wing-fuselage interference on $C_l'_{\psi}$ and $C_n'_{\psi}$ due to the tail is isolated from the effect of center-of-gravity location.

The pitching-moment coefficient was not zero for most of the tests. A correction to $C_l'_{\psi}$ should be made by means of the following formula:

$$C_{l\psi} = C_l'_{\psi} + 0.0029 C_m$$

DISCUSSION

General comments.— The movement of the center of gravity of the model with change in wing location results in a change in the slope of the pitching-moment curves, as may be seen in figure 3. Inasmuch as the pitching moment of the fuselage becomes more stable as the center of gravity is moved forward, the forward-wing arrangements are expected to be more stable in pitch than the rearward-wing arrangements.

The effect of the fillet on the characteristics of the low-rearward arrangement (figs. 3(f) and 3(g)) is of interest. The fillet prevents separation below the normal stall and thus increases the maximum lift coefficient and smooths the breaks in the curves of drag and pitching-moment coefficient. It may be noted, however, that the angle of attack for maximum lift is higher without the fillet when the flap is undeflected.

In the plots of the yaw tests at high angles of attack (figs. 4 to 6), the effects of center-of-gravity location and fillet are again in evidence. With the vertical tail in place the forward-wing combinations are most stable in yaw because of the longer tail length. The fillet on the low-reward combination reduces a large variation of C_l'

with ψ' to practically zero by removing the effect of the burble. The effect of the center-of-gravity location and the fillet will be discussed in greater detail in later sections.

The lateral-stability characteristics of the fuselage and the wing shown in figure 7 are reproduced from references 4 and 5.

Wing-fuselage interference.— The effects of vertical position of the wing on the fuselage on lateral stability characteristics have already been discussed in reference 4; hence the discussion in this report will be confined chiefly to the effects of changing the wing position longitudinally along the fuselage. The effect of vertical position of the wing is, however, about the same regardless of longitudinal location.

The increment $\Delta_1 C_{l'} \psi$ (shown in figs. 8 and 14) is positive for the high-wing combinations and negative for the low-wing combinations. Variations with longitudinal changes in wing location are small. If the low wing with flaps neutral is moved either forward or rearward, there is a small increase in effective dihedral. The increase, however, is not enough to make $\Delta_1 C_{l'} \psi$ positive. For all wing positions with flaps deflected 60° there is, in general, a decrease in effective dihedral as the wing is moved in either direction from center; the decrease is greater for movement forward. The fillet on the low-rearward combination with $\delta_f = 0^\circ$ (fig. 8(c)) removes the break and the reversal of sign caused by the burble at 10° angle of attack.

The parameter $\Delta_1 C_{n'} \psi$ (figs. 9 and 14) has a tendency to become more stabilizing as the wing moves forward, although the trend is not consistent, especially in the case of the low-wing combination. The contours (fig. 14) show an increase in the stabilizing influence of $\Delta_1 C_{n'} \psi$ as the wing is moved forward, particularly when $\delta_f = 60^\circ$, but the tendency does not hold for the entire unstalled angle-of-attack range. As in the case of $\Delta_1 C_{l'} \psi$, the fillet prevents the sudden divergence of $\Delta_1 C_{n'} \psi$ at high angles of attack caused by flow separation at the wing root.

When $\Delta_1 C_n'_{\psi}$ is recalculated for center-of-gravity location fixed at the central position on the fuselage, the foregoing effects are not apparent or are even reversed in some cases (figs. 9(d) and 9(e)).

The value of $\Delta_1 C_Y'_{\psi}$ is usually positive but is small for midwing combinations (figs. 10 and 14). With flaps neutral, movement of the wing either forward or rearward has very little effect, but the tendency is toward a decrease in $\Delta_1 C_Y'_{\psi}$. With flaps deflected 60° , movement of the wing in any direction from the midcenter position increases the lateral force due to interference for angles of attack of normal flight. When the wing is in the high or the low position, it probably acts as a partial end plate, increasing the effective aspect ratio of the fuselage that is acting as an airfoil when yawed; hence, an increase in lateral force is to be expected.

Effect of wing-fuselage interference on vertical tail.— The increment $\Delta_2 C_l'_{\psi}$ is shown in figures 11 and 15, where the effect of longitudinal position of the wing is seen to be small and erratic.

In general, $\Delta_2 C_n'_{\psi}$ (figs. 12 and 15) is positive, or destabilizing, for the high-wing combinations and is negative, or stabilizing, for the low-wing combinations. The longitudinal position of the wing has little effect. In most cases, the increment $\Delta_2 C_n'_{\psi}$ becomes more stabilizing as the wing is moved rearward along the fuselage. With flaps neutral, the fillet decreases the directional stability at low and medium angles of attack but produces no change at high angles below the stall. With flaps deflected 60° , the fillets increase the directional stability and the variation is less erratic at high angles of attack.

When moments based on a fixed tail length are considered, there is a small but definite tendency toward an increase in interference as the wing is moved rearward. This interference is destabilizing for the case of the high wing and is stabilizing for the case of the low wing (figs. 12(d) and 12(e)).

In general, $\Delta_2 C_Y'_{\psi}$ (figs. 13 and 15) is positive for the low-wing combinations and negative for the high-

wing combinations. The effect is small, but the trend is toward more interference as the wing is moved rearward, which decreases the lateral force of the high-rearward combination and increases the lateral force of the low-rearward combination (figs. 13(a) and 13(c)). The contours (fig. 15), however, show that this effect may be chiefly caused by the fact that the forward wings are closer to the center line of the fuselage. With flaps deflected 60° , the fillet increases the lateral force on the vertical tail. At high angles of attack there is also an increase with the flaps neutral.

Some of the relations between $\Delta_2 C_n' \psi$ and $\Delta_2 C_y' \psi$ are of interest. The existence of sidewash angles in the region of the vertical tail for a model very similar to the present one was reported in reference 9. For the low-wing combination the sidewash angles increased the directional stability, while for the high-wing combinations the sidewash angles decreased the directional stability. Since the present report shows that the rearward wings have an even greater influence on the vertical tail, there must be an increase in the sidewash angles. A comparison of $\Delta_2 C_n' \psi$ and $\Delta_2 C_y' \psi$ with and without the fillet for the low-rearward combination shows that, in general, the fillet causes a forward shift in the lateral center of pressure.

CONCLUSIONS

The effect of changing the wing position longitudinally on the fuselage was small when compared with the effect of changing the wing position vertically. For the low-wing combinations with flap neutral, there was a small increase in effective dihedral as the wing position was shifted in either direction longitudinally from the central position. For all combinations with flaps deflected 60° , the effective dihedral decreased as the wing was moved longitudinally in either direction from the central position.

The change in directional stability due to interference with change in the longitudinal position of the wing was small, but the wing-fuselage interference tended to increase the directional stability as the wing was moved from the rearward position to the forward position. The influence of the wing-fuselage interference on the vertical

tail was slightly greater for the rearward wing positions than for the forward positions. The tendency was to make the high-wing combination less stable directionally and the low-wing combination more stable directionally.

For tailless combinations with flaps neutral, changes in lateral force caused by longitudinal position of the wing were negligible. For all combinations with flaps deflected 60° , the wing-fuselage interference tended to increase the lateral-force coefficient. The lateral force became greater as the wing was moved in any direction from the midcenter position. The influence of wing-fuselage interference on the vertical tail was slightly greater for the rearward-wing combinations than for the forward combinations. The interference tended to reduce the lateral-force coefficient for the high-rearward combination and to increase it for the low-rearward combination.

A fillet at the wing-fuselage juncture on the low-rearward combination removed the effect of the burble and prevented the sharp divergence of lateral-stability characteristics a few degrees below complete wing stall. Its effect at low angles of attack was generally small.

The wing location giving most favorable total interference for the low-wing combinations was the rearward position; for the high-wing combinations it was the forward position.

Langley Memorial Aeronautical Laboratory,
National Advisory Committee for Aeronautics,
Langley Field, Va., July 31, 1941.

REFERENCES

1. Shortal, Joseph A.: Effect of Tip Shape and Dihedral on Lateral-Stability Characteristics. Rep. No. 548, NACA, 1935.
2. Bamber, M. J., and House, R. O.: Wind-Tunnel Investigation of Effect of Yaw on Lateral-Stability Characteristics. I - Four N.A.C.A. 23012 Wings of Various Plan Forms with and without Dihedral. T.N. No. 703, NACA, 1939.
3. Pearson, Henry A., and Jones, Robert T.: Theoretical Stability and Control Characteristics of Wings with Various Amounts of Taper and Twist. Rep. No. 635, NACA, 1938.
4. House, Rufus O., and Wallace, Arthur R.: Wind-Tunnel Investigation of Effect of Interference on Lateral-Stability Characteristics of Four NACA 23012 Wings, an Elliptical and a Circular Fuselage, and Vertical Fins. Rep. No. 705, NACA, 1941.
5. Bamber, M. J., and House, R. O.: Wind-Tunnel Investigation of Effect of Yaw on Lateral-Stability Characteristics. II - Rectangular N.A.C.A. 23012 Wing with a Circular Fuselage and a Fin. T.N. No. 730, NACA, 1939.
6. Harris, Thomas A.: The 7 by 10 Foot Wind Tunnel of the National Advisory Committee for Aeronautics. Rep. No. 412, NACA, 1931.
7. Wenzinger, Carl J., and Harris, Thomas A.: Wind-Tunnel Investigation of an N.A.C.A. 23012 Airfoil with Various Arrangements of Slotted Flaps. Rep. No. 664, NACA, 1939.
8. Jacobs, Eastman N., and Ward, Kenneth E.: Interference of Wing and Fuselage from Tests of 209 Combinations in the N.A.C.A. Variable-Density Tunnel. Rep. No. 540, NACA, 1935.
9. Recant, Isidore G., and Wallace, Arthur R.: Wind-Tunnel Investigation of the Effect of Vertical Position of the Wing on the Side Flow in the Region of the Vertical Tail. T.N. No. 804, NACA, 1941.

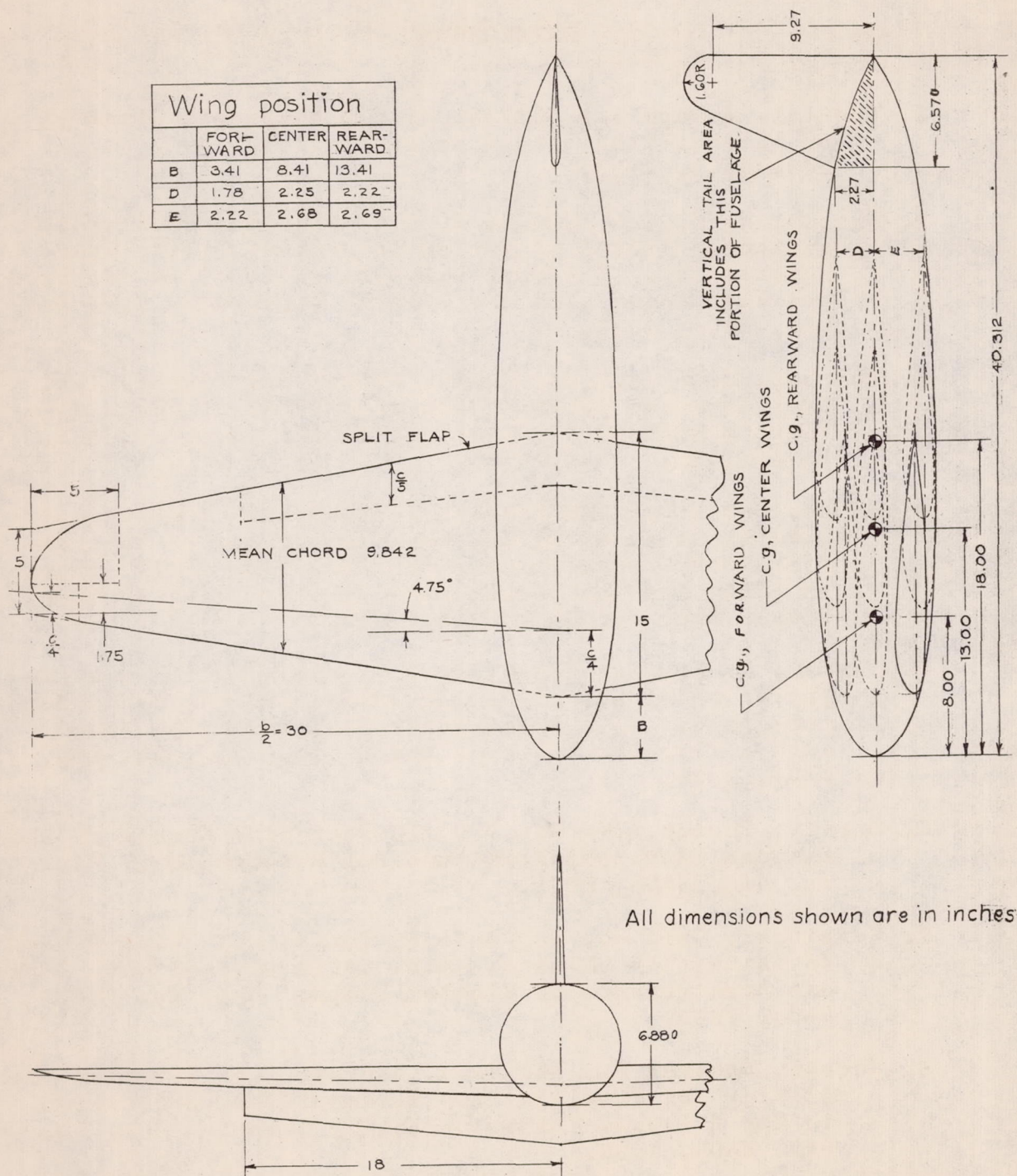


Figure 1. Drawing of NACA 23012 wing in combination with circular fuselage and fin of NACA 0009 section.

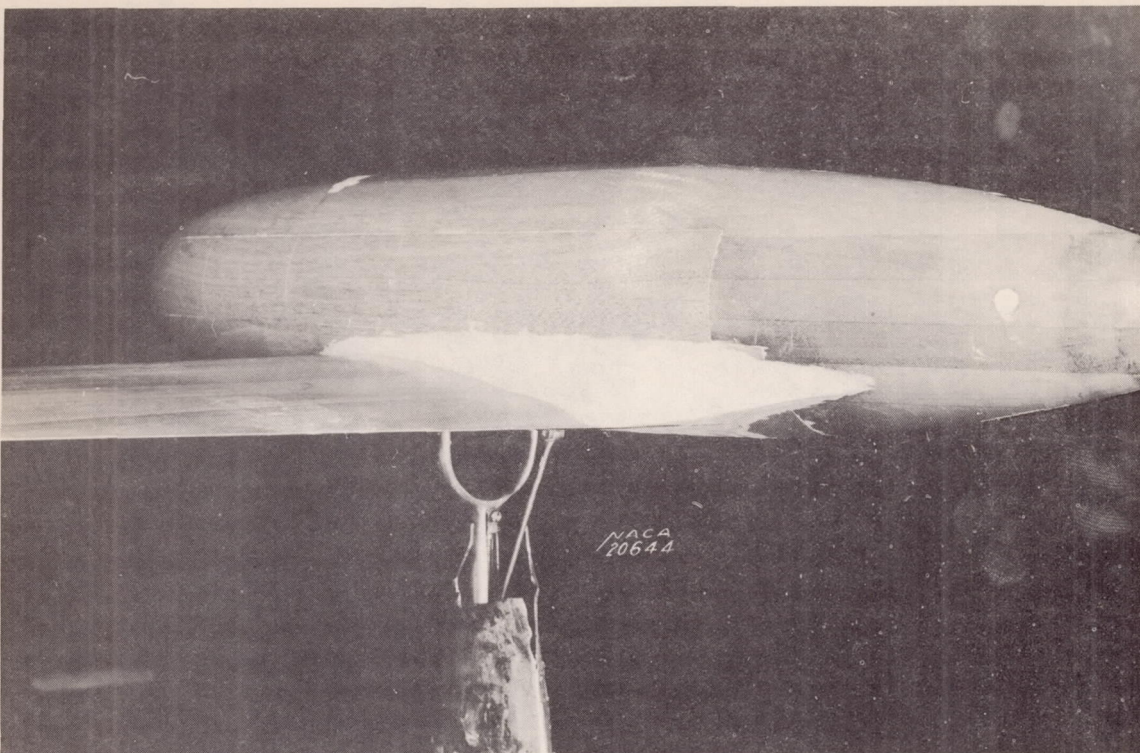
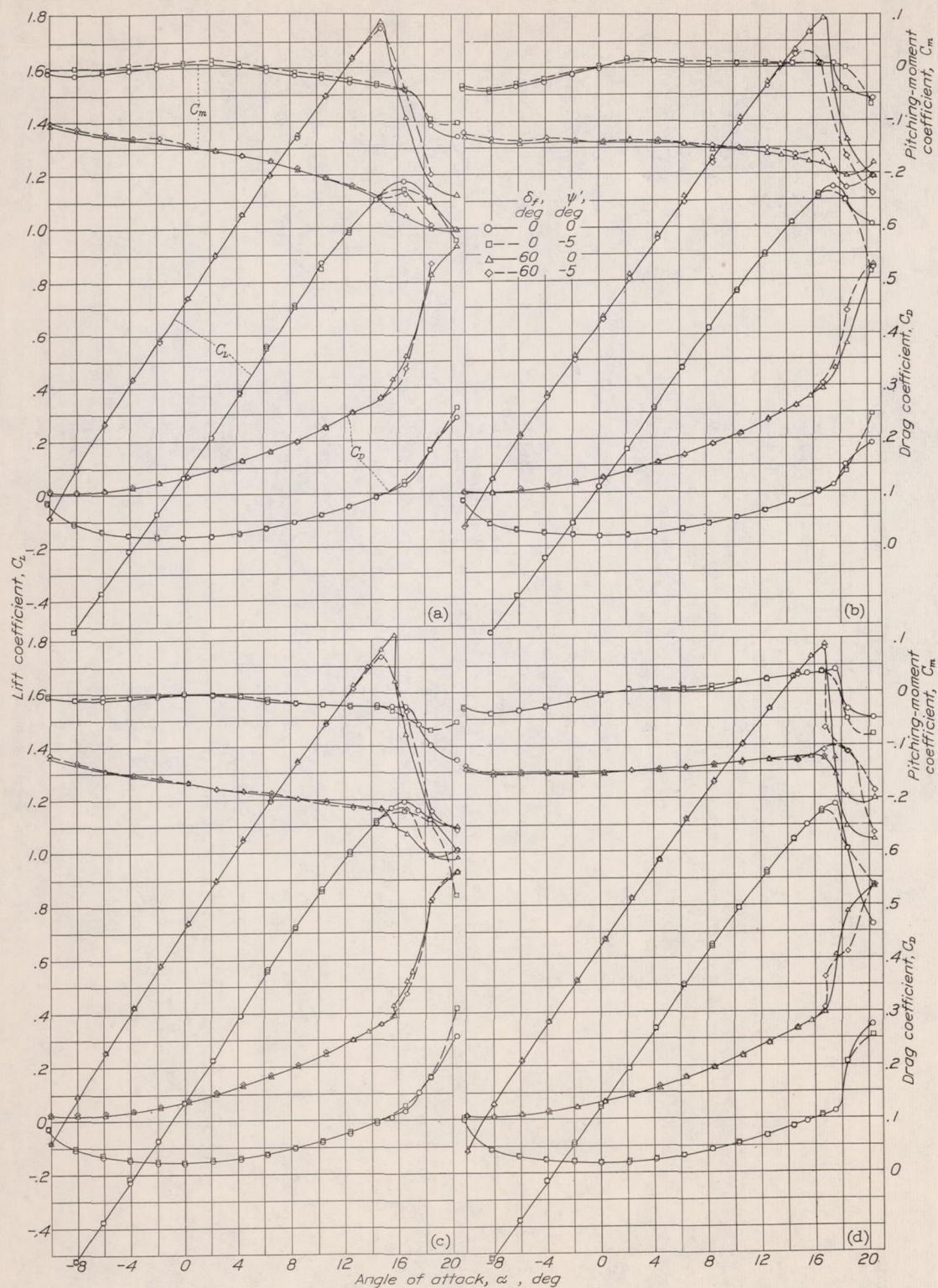


Figure 2a.- Rear view of wing fillet on low-wing monoplane model tested in the NACA 7- by 10- foot wind tunnel.



Figure 2b.- Side view of wing fillet on low-wing monoplane model tested in the NACA 7- by 10- foot wind tunnel.



(a) Wing forward and high. (b) Wing rearward and high. (c) Wing forward and middle. (d) Wing rearward and middle.

Figure 3 a to g.- Lift, drag, and pitching-moment coefficients of the complete model NACA 23012 wing with circular fuselage and fin.

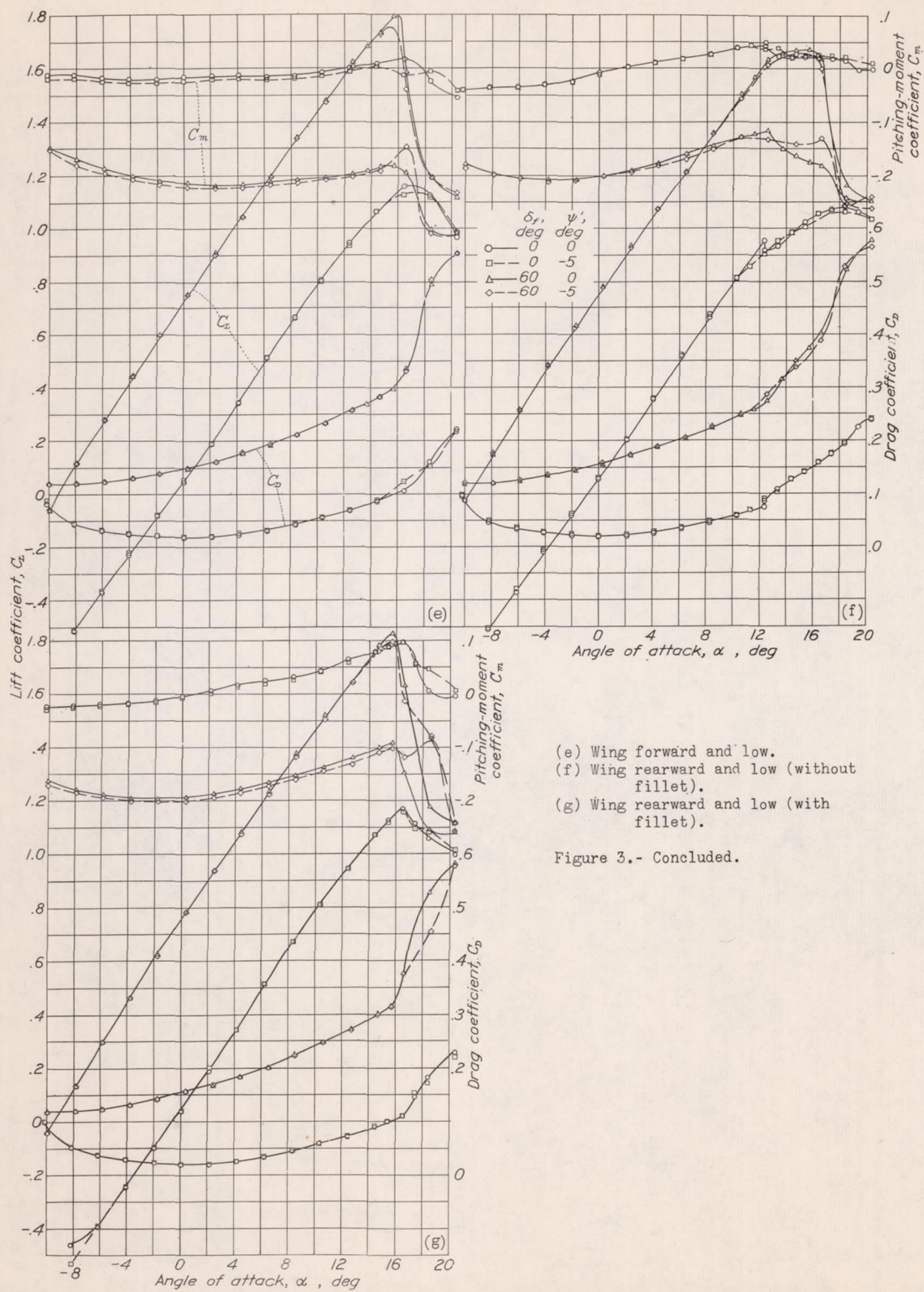


Figure 3.- Concluded.

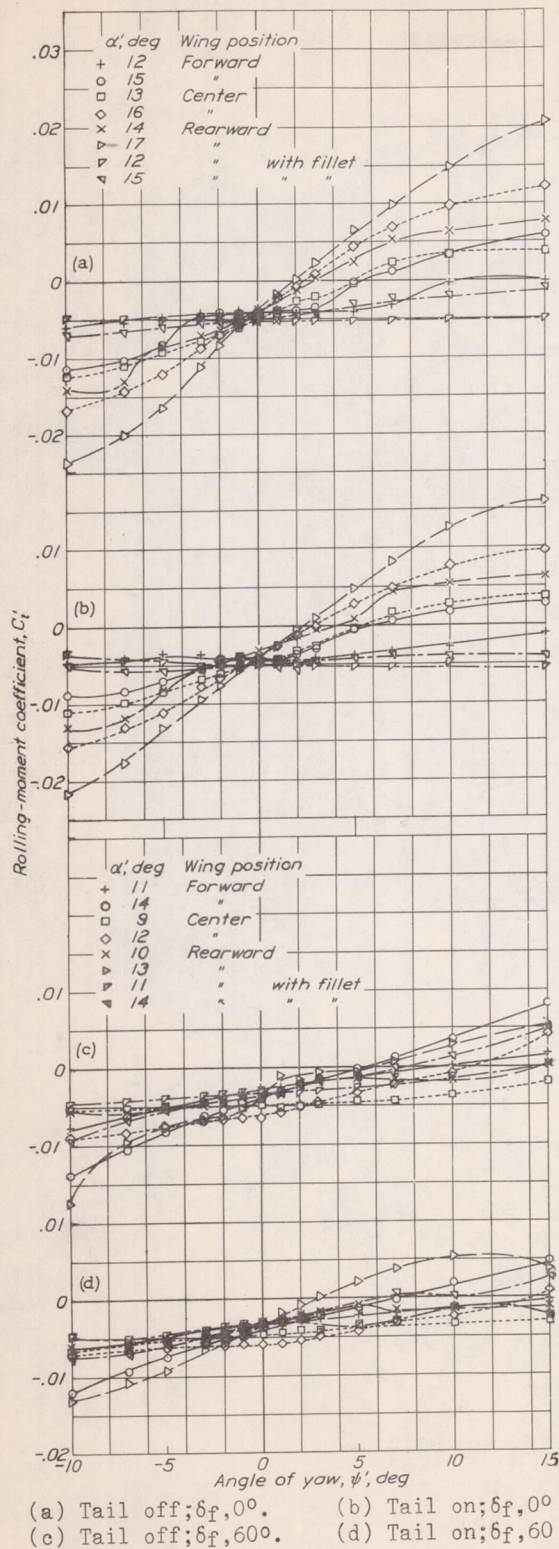


Figure 4.- Variation of rolling-moment coefficient with yaw. NACA 23012 wing with circular fuselage as low-wing monoplane.

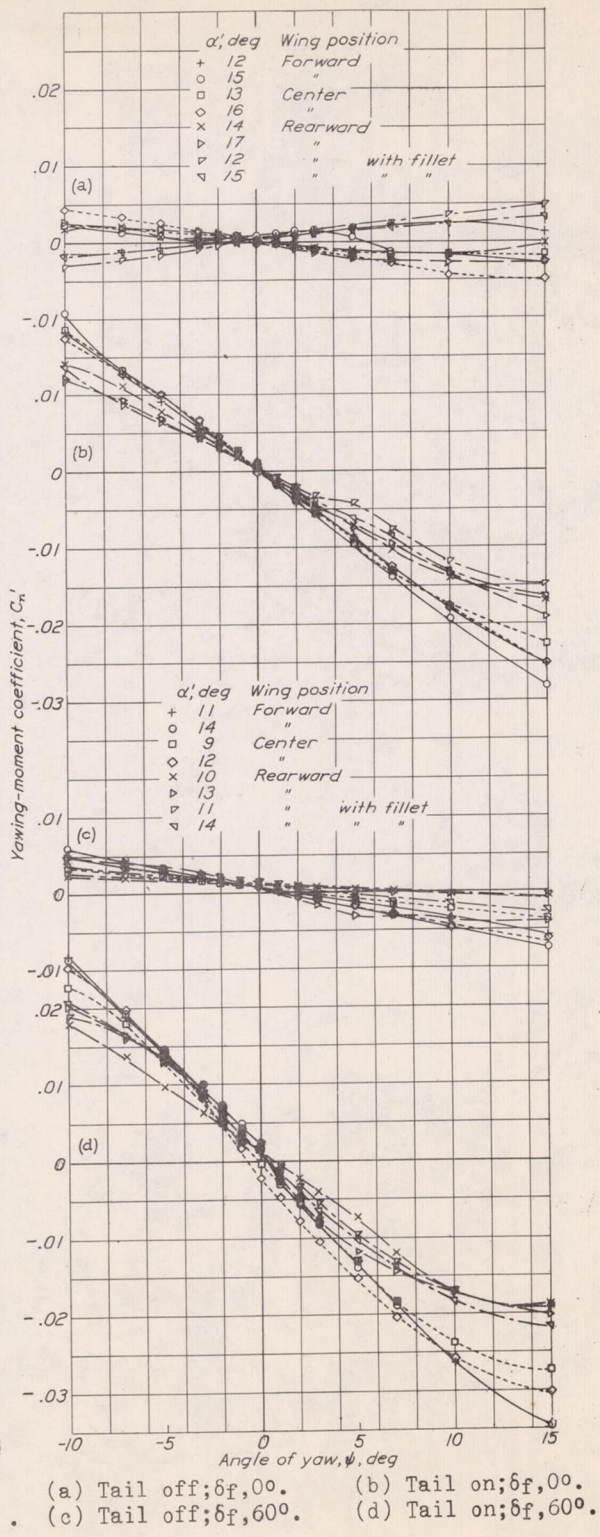


Figure 5.- Variation of yawing-moment coefficient with yaw. NACA 23012 wing with circular fuselage as low-wing monoplane.

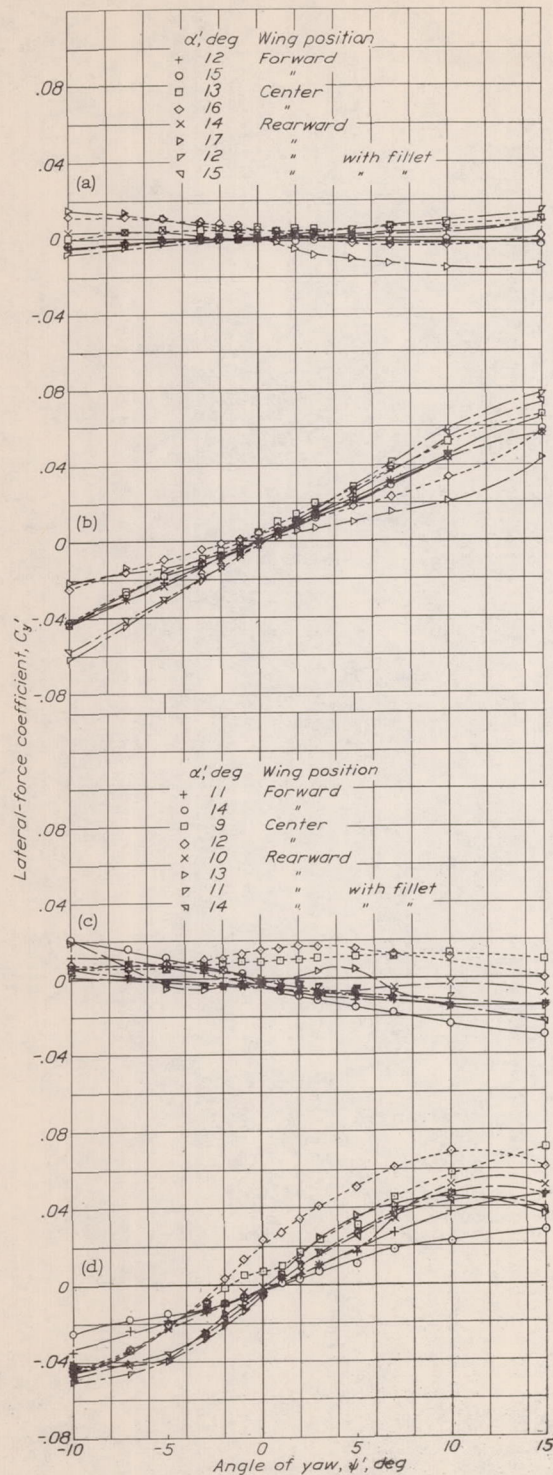


Figure 6.- Variation of lateral-force coefficient with yaw. NACA 23012 wing with circular fuselage as low-wing monoplane.

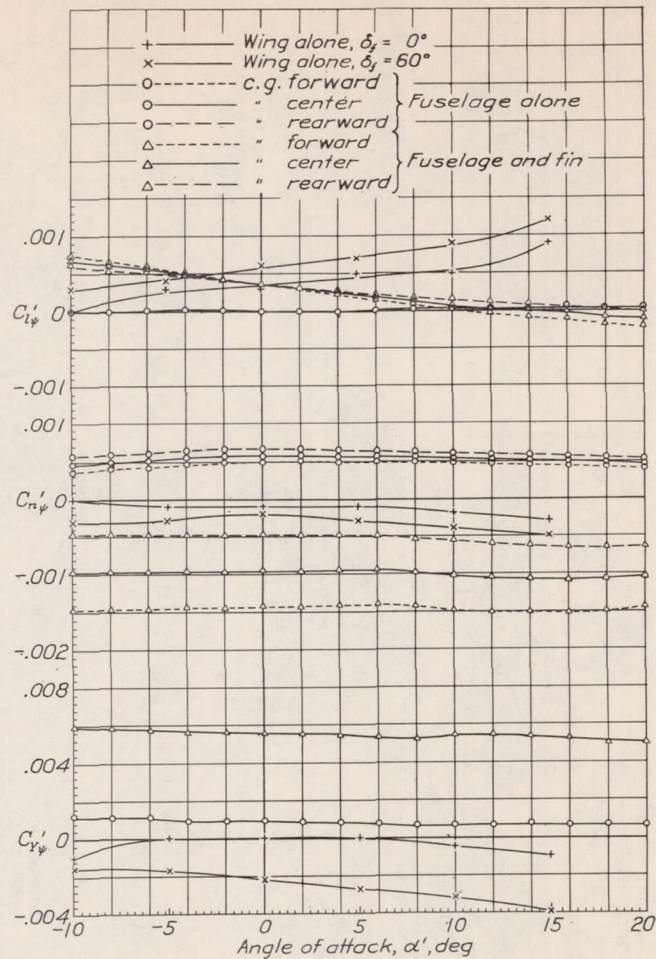


Figure 7.- Variation of $C_{l'}$, $C_{n'}$, and $C_{y'}$ with angle of attack. NACA 23012 wing alone, circular fuselage alone, and circular fuselage with fin. (Data from references 4 and 5).

Figure 8.- Increment of $C_{L\downarrow}$ due to wing-fuselage interference. NACA 23012 wing with circular fuselage.

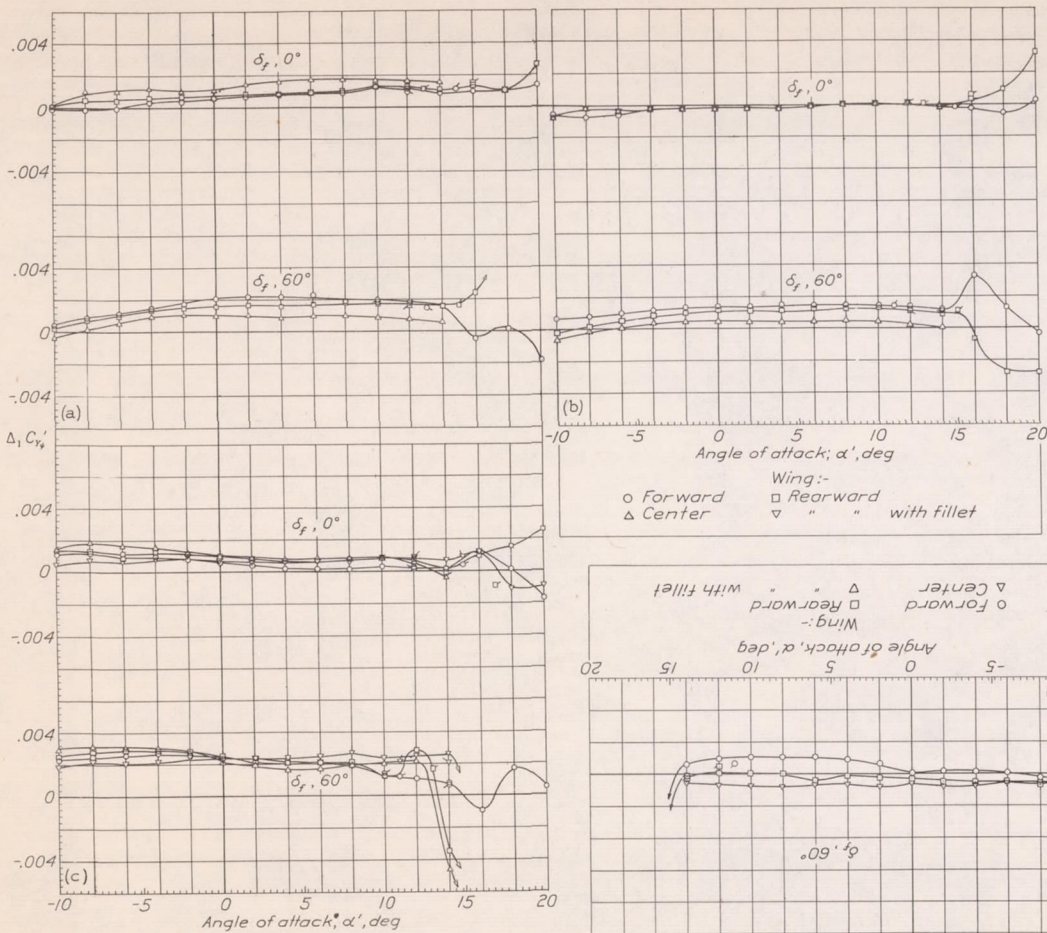
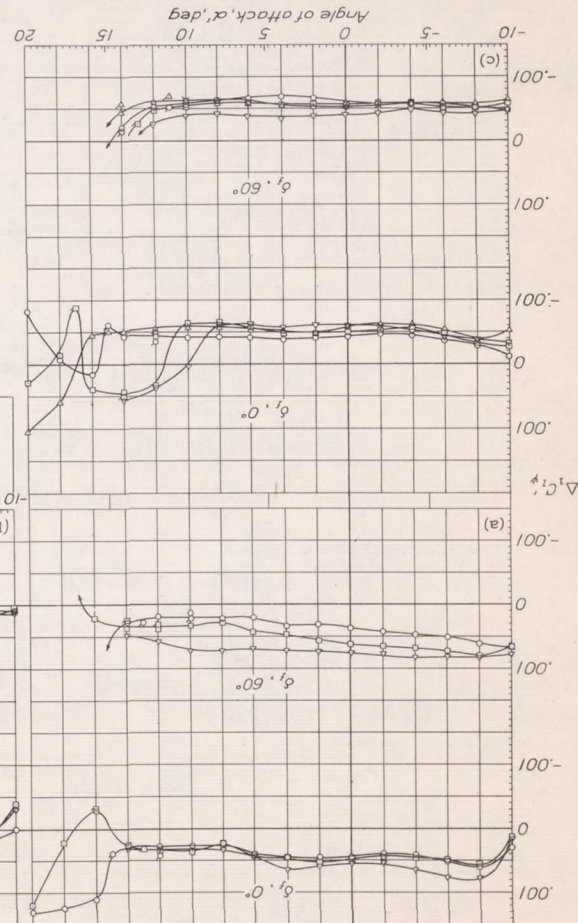
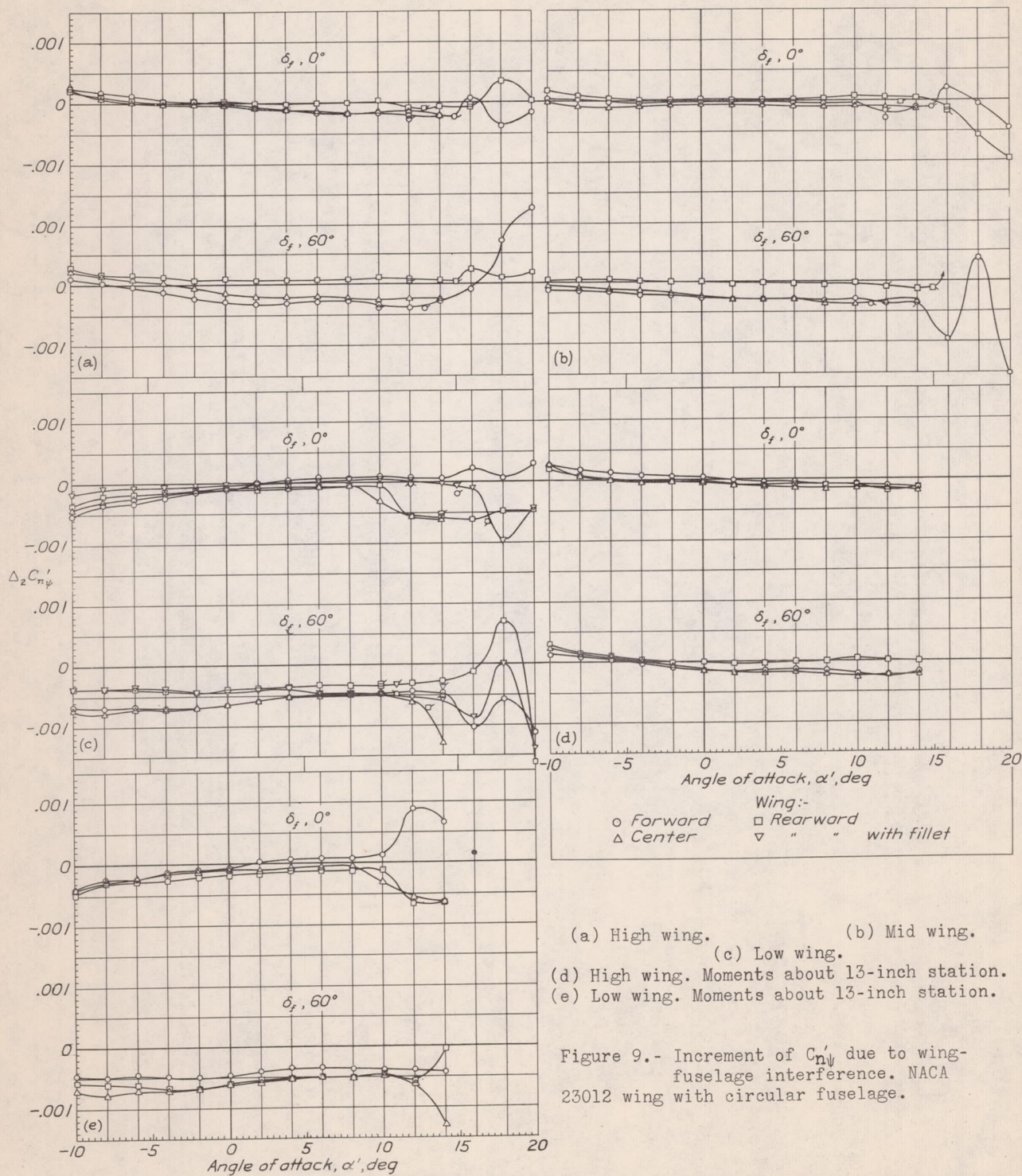
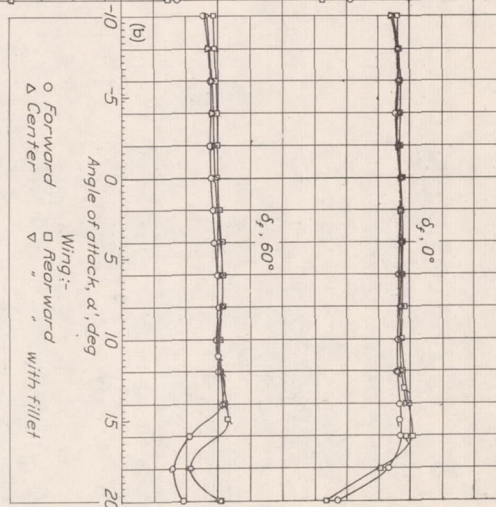
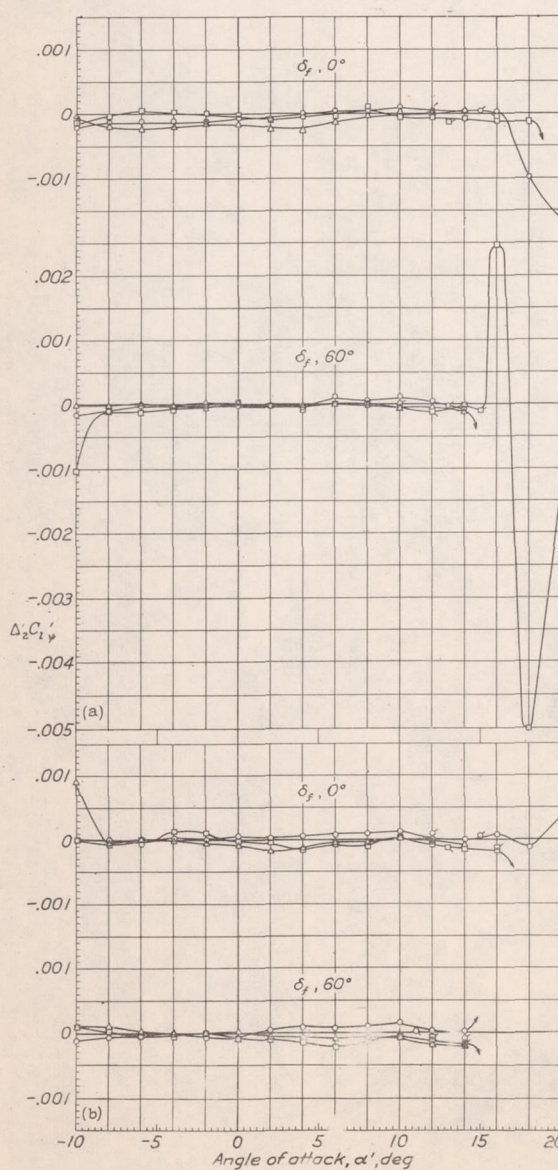
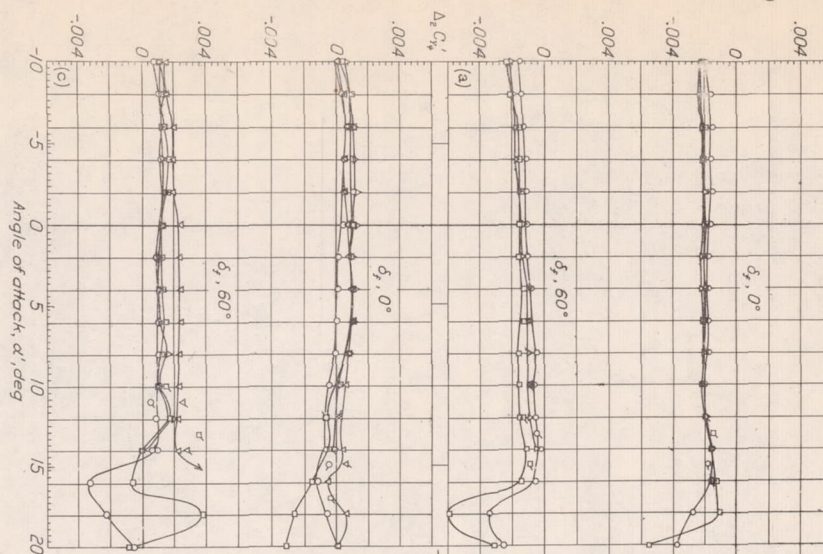


Figure 10.- Increment of $C_{Y\downarrow}$ due to wing-fuselage interference. NACA 23012 wing with circular fuselage.

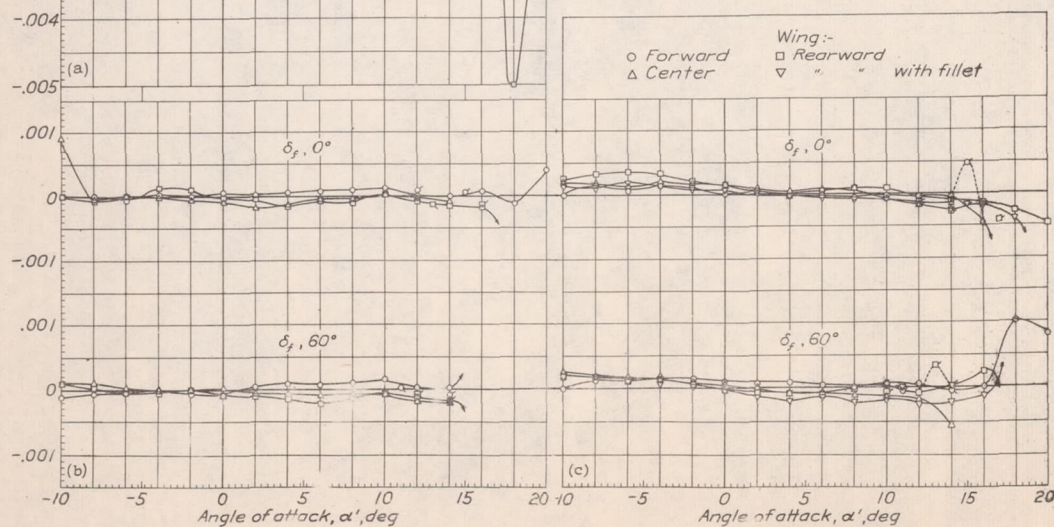


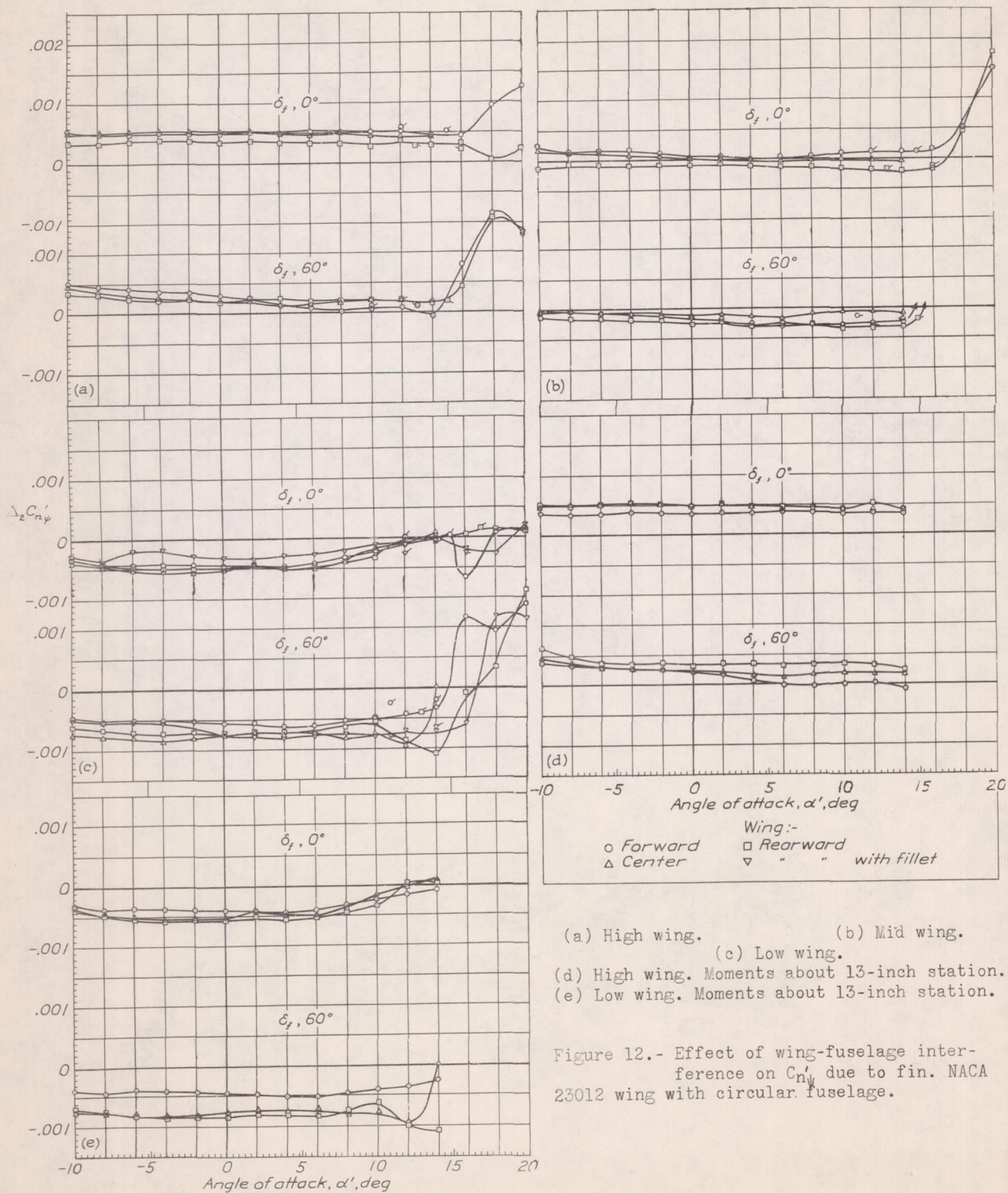
(a) High wing. (b) Mid wing. (c) Low wing.
Figure 13.- Effect of wing-fuselage interference
on C_{Yf} due to fin. NACA 23012 wing
with circular fuselage.



(a) High wing. (b) Mid wing. (c) Low wing.

Figure 11.- Effect of wing-fuselage interference
on C_{L_f} due to fin. NACA 23012 wing
with circular fuselage.





(a) High wing. (b) Mid wing.
(c) Low wing.
(d) High wing. Moments about 13-inch station.
(e) Low wing. Moments about 13-inch station.

Figure 12.- Effect of wing-fuselage interference on $C_{n'}$ due to fin. NACA 23012 wing with circular fuselage.

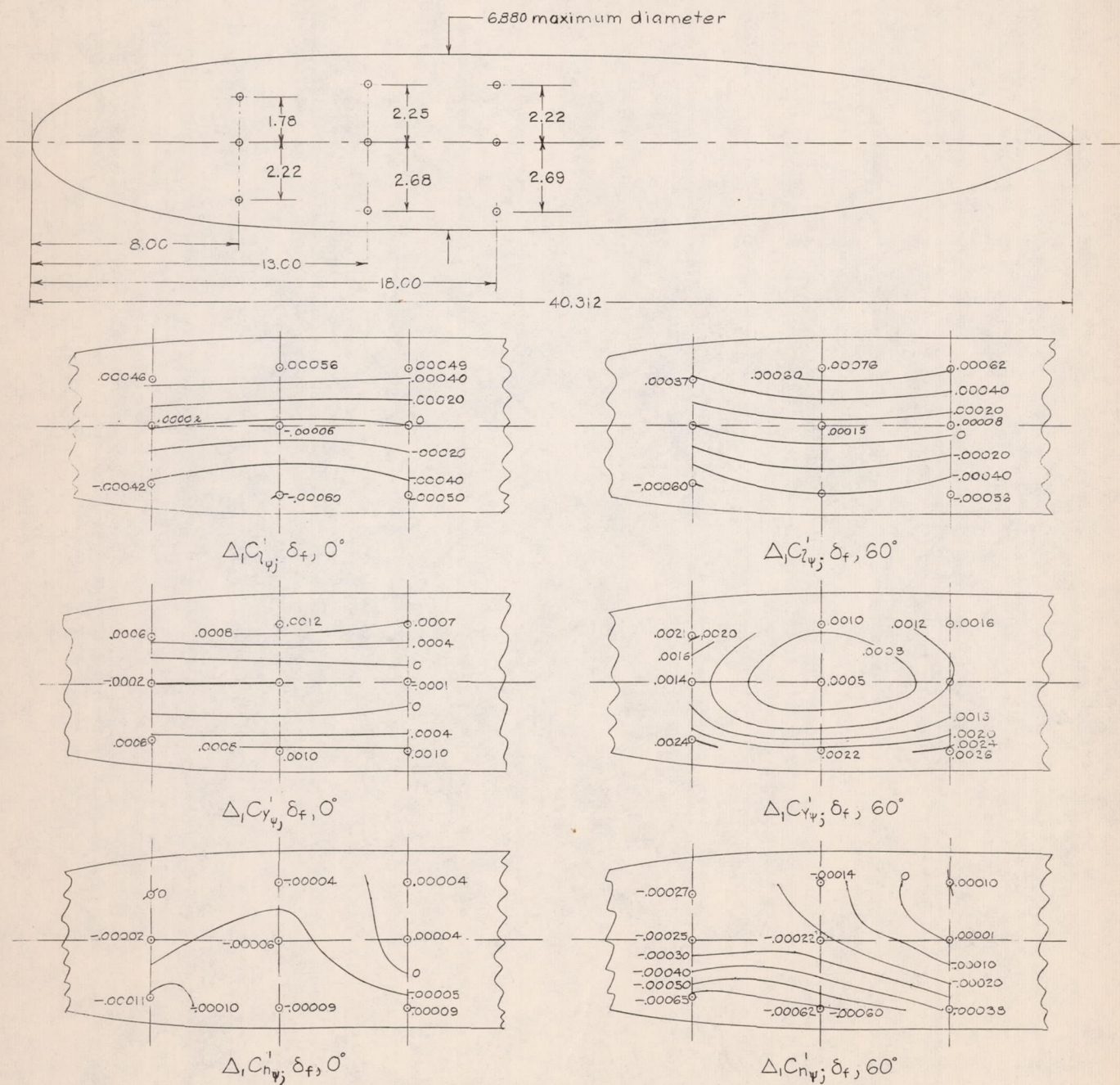


Figure 14.—Contours of location of wing aerodynamic center for increments of C_L' , C_Y' , and C_N' due to wing-fuselage interference. NACA 23012 wing and circular fuselage; $\alpha', 0^\circ$.

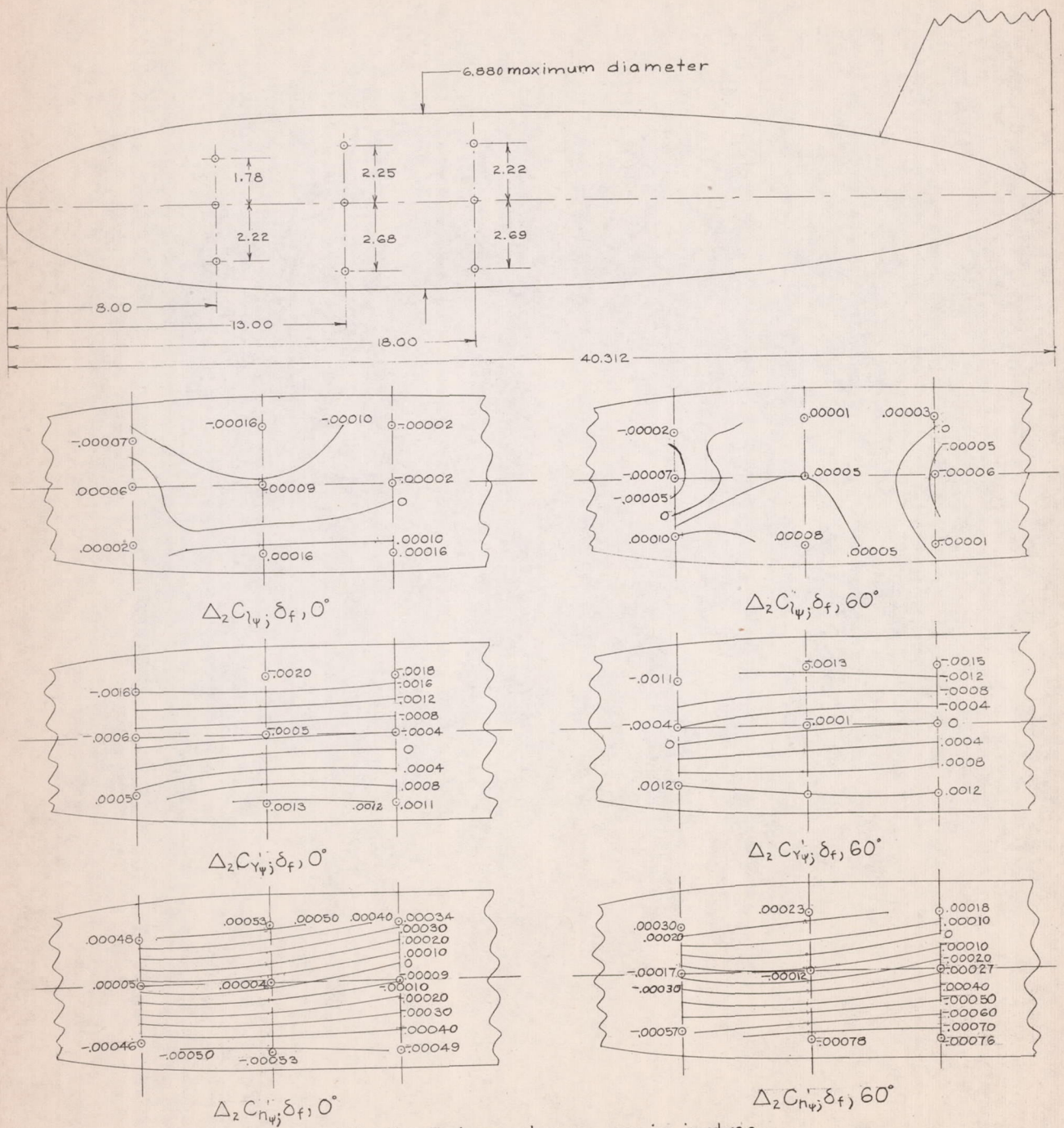


Figure 15.-Contours of location of wing aerodynamic center showing effect of wing-fuselage interference on $C_{l\psi}'$, $C_{Y\psi}'$, and $C_{N\psi}'$ due to fin. NACA 23012 wing and circular fuselage and fin; $\alpha'_i, 0^\circ$.